JUNCTION RIEMANN PROBLEM FOR 1-D SHALLOW WATER EQUATIONS WITH BOTTOM DISCONTINUITIES AND CHANNELS WIDTH VARIATIONS

MOHAMED ELSHOBAKI

Department of Information Engineering, Computer Science, and Mathematics
University of L'Aquila, 67010, L'Aquila, Italy
mohabd@univaq.it

ALESSANDRO VALIANI

Department of Engineering
University of Ferrara, 44122 Ferrara, Italy
alessandro.valiani@unife.it

VALERIO CALEFFI

Department of Engineering
University of Ferrara, 44122 Ferrara, Italy
valerio.caleffi@unife.it

Received (14 Nov. 2016)

Abstract. In this paper, we investigate the solution of the nonlinear junction Riemann problem for the one dimensional shallow water equations in a simple star network of three rectangular channels, by considering possible bottom discontinuities between the channels and possible differences in the channels width. In the literature, the solution of the Riemann problem at the junction is investigated for the symmetric case without bottom steps and channels width variations. Here, the solution is extended to a more general case, such that neither equality of the channels width nor symmetric flow have assumed in the downstream channels. All the analysis are performed under sub-critical flow conditions. The results are summarized in a Theorem, and series of numerical examples are considered to support our findings.

Keywords: Shallow water equations; Riemann problem; junction network.

1. Introduction

Nowadays, mathematical models for network flows constituted by partial differential equations (PDEs) are well defined (e.g. well posedness, existence, and uniqueness) [1]. Many applications benefit from this property. Typical examples are free surface flow in irrigation systems or natural rivers, traffic flow, and blood flow [2–4]. In particular, open channel flow in networks is of great interest from the environmental-hydraulic perspective. The simplest form of channels network is a star network. It consists of three rectangular channels joined at a junction node. Providing realistic

conditions at the junction node is therefore a crucial point to characterize the water flow in such system.

The one dimensional shallow water equations (SWE) are well established for simulation of open channel flow in both sub-critical and super-critical flow [5]. However, using SWE in open channels network is not a trivial target because the junction node is a singular point for the SWE [6]. Therefore implementing one dimensional simulation in such networks requires internal boundary conditions, which are defined as functions dependent on the solution, to connect the channels at each junction node.

In the last decade, the use of the one dimensional SWE for the simulations of open channels network has been presented in several works, see for examples [7–12]. Avoiding the ill-possedness of the used mathematical model, six unknowns (three water depths and three water discharges) must computed at the junction node, providing the internal boundary conditions, and therefore the mathematical model is well possed. Hence, six relationships have to be defined, forming a nonlinear system that is numerically solved at each time step to provide the inner boundary conditions. In the case of sub-critical flow [9, 11, 12], three relationships are obtained by using the characteristics curves [13–15], the fourth relationship is obtained by assuming the mass continuity at the junction node [6], the two remaining relationships are obtainable by one of the following junction models; Equality model [16], Gurram model [17], Hsu model [18], and Shabayek model [19]. Equality model is derived by using equality of specific energy at the junction and it is simplified to equality of flow depths by neglecting the velocity head at the junction node [16]. Gurram model is derived by applying momentum conservation principle and take into account the junction angle. Hsu model is similarly derived as Gurram model but with energy and momentum correction factors. Shabayek model is a general nonlinear model based on the theory that involves most of the physical phenomena at the junction. In the case of super-critical flow [11, 12], four relationships are obtained by using the characteristics curves [13–15], the fifth relationship is obtained by assuming mass continuity at the junction [6], the remaining relationship is obtained by the Rice super-critical junction model [20] or a non-linear dynamical equation with momentum conservation [21–23]. However, these junction model are used by Engineers without mathematical evidences that guarantee the existence and uniqueness of the generated solutions.

Indeed, using further mathematical analysis, a recent approach for computing the internal boundary conditions is defined on a proper extension of the Riemann problem. This approach is based on the theoretical background provided in [24] and is numerically verified by Briani et al. [1]. The Riemann solution of SWE in one dimension is thoroughly investigated in [25–27] with or without bottom discontinuties. A well posed Cauchy problem for P-system at the junction is established in [28] and then in [29] is extended to define the Riemann problem for 2x2 conservation laws at the junction. Goudiaby et al. [24] provides the mathematical tools for establishing a unique solution of the nonlinear junction Riemann problem of 1-D SWE in a star-

like network of three channels. Mass conservation and equality of energy levels at the junction are assumed. The flow is assumed to be symmetric in the downstream channels and sub-critical along the network.

Here, our analysis consideres the results by Goudiaby et al. [24] and by implementing the nonlinear junction Riemann Problem of 1-D SWE, we face a more general case. In particular, no assumptions of symmetry or equal channels width are considered and bottom discontinuities between the channels at the junction are taken into account. The conservation of mass and the total head equality at the junction are used as a consequance of the steady state solution of the SWE, more details about the total head physical meaning can be found in [30]. The flow in the three channels are assumed to be sub-critical. The Riemann solution is geometrically presented by finding the intersection points of certain curves in phase space. These curves are *Hugoniot loci* [32], Integral curves [32], and junction curves. The junction curves are defined by using mass conservation and total head equality, whilst the physical domains of the non-dimensional SWE variables are of great help. Several situations where no solution to the Riemann problem can be found, are investigated.

The rest of paper is organized as follow: In Section 2, a brief discussion of the shallow water equations is presented. The solution structure of the junction Riemann problem is shown in Section 3. In Section 4, some examples to support the findings of the previous section are presented. Lastly, in Section 5 we conclude with some discussions on the results.

2. The shallow water equations and its standard Riemann problem

2.1. *The shallow water equations*

The one dimensional shallow water equations, also known as Saint Venant equations, are defined as a mathematical model to describe open channel flow by considering the vertical depth small with respect to the horizontal length scale. SWE are a particular case of Navier- Stokes equations, obtained by integrating the mass and momentum equations over the depth. The SWE can be written in a conservative form as:

$$\frac{\partial U}{\partial t} + \frac{\partial F}{\partial x} = S, \quad \text{in } [0, L], \tag{2.1}$$

with

$$U = \begin{bmatrix} h \\ hu \end{bmatrix}, \quad F = \begin{bmatrix} hu \\ hu^2 + \frac{gh^2}{2} \end{bmatrix}, \quad S = \begin{bmatrix} 0 \\ -gh(S_0 - S_f) \end{bmatrix}, \tag{2.2}$$

where u and h are the flow velocity and flow depth, respectively. L is the channel length; g is the gravity acceleration; $S_o = -\frac{\partial z}{\partial x}$ is the bed slope and z is the bottom elevation; S_f is the friction slope. Since the Riemann solution is asociated to the frictionless cases [25], then the friction slope can be neglected and therefore it is

assumed here to be equal to zero. A non-zero bottom elevation is considered. Equation (2.1) can be cast in a quasi-linear form. Then we have

$$\frac{\partial v}{\partial t} + A(v)\frac{\partial v}{\partial x} = 0, \quad \text{in } [0, L], \tag{2.3}$$

with

$$v = \begin{bmatrix} h \\ hu \\ z \end{bmatrix}, \quad A(v) = \begin{bmatrix} 0 & 1 & 0 \\ c^2 - u^2 & hu & gh \\ 0 & 0 & 0 \end{bmatrix}. \tag{2.4}$$

The matrix A has three real distinct eigenvalues λ_j with $j = 1, 2, 3$.

$$\lambda_1(v) = u - c, \quad \lambda_2(v) = u + c, \quad \lambda_3(v) = 0, \tag{2.5}$$

where $c = \sqrt{gh}$ is the wave celerity. A very important parameter for the shallow water equations is the Froude number $Fr = \frac{u}{c}$. The flow is sub-critical if $Fr < 1$, critical if $Fr = 1$, and super-critical if $Fr > 1$. The critical curves are defined as follow

$$C^+ := \{q = h\sqrt{gh}\}, \quad C^- := \{q = -h\sqrt{gh}\}, \tag{2.6}$$

respectively; $q = hu$ is the specific discharge. On the critical curves the left and the

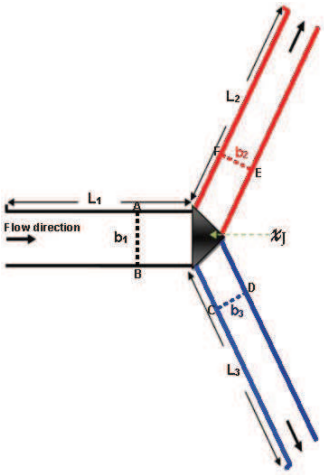

Fig. 1. Star-Network of three rectangular channels.

right eigenvalues (i.e., λ_1 and λ_2, respectively) coincide with the third eigenvalue λ_3. In this condition the SWE lose their hyperbolicity and therefore system (2.3) is not a strictly- hyperbolic system [27]. On the other hand, under sub-critical flow conditions the system is always strictly hyperbolic and the theory of hyperbolic systems can be used. In the natural open channels networks, the Fr number is generally small therefore, considering only Fr numbers smaller than 1 does not

limit the practical utility of this analysis. Thus, for simplicity we restrict ourselves to sub-critical flow conditions for the rest of the paper.

2.2. *Standard Riemann problem*

Assuming a constant bottom elevation, the system (2.3) can be used to define the standard Riemann problem for a single channel. We consider the following initial piecewise constant states

$$v(0,x) = \begin{cases} v_l & \text{if} \quad x < 0 \\ v_r & \text{if} \quad x > 0 \end{cases} \tag{2.7}$$

where v_l and v_r are the left and right initial condition, respectively. In the sub-critical conditions, the solution consists of two unperturbed states and an intermediate state separated by a left wave and a right wave [27]. The intermediate state is connected to the left unperturbed state through a shock or a rarefaction, and is connected to the right unperturbed state through a shock or rarefaction. Therefore, the intermediate state are defined by using the *Rankine Hugoniot loci* and Riemann integral curves as it is shown in the next subsection.

2.3. *Left and right wave curves*

The *Hugoniot loci* and integral curves are combined to define the left wave curve (τ_l-curve) and the right wave curve (τ_r- curve). First, we introduce the functions β_l and β_r as:

$$\beta_l(h_o; v_l) = q_o = R_l(h_o, v_l) \cup S_l(h_o, v_l) = \begin{cases} R_l(h_o; v_l), \text{ if } h_o < h_l, \\ S_l(h_o; v_l), \text{ if } h_o > h_l, \end{cases} \tag{2.8}$$

and

$$\beta_r(h_o; v_r) = q_o = R_r(h_o, v_r) \cup S_r(h_o, v_r) = \begin{cases} R_r(h_o, v_r), \text{ if } h_o < h_r, \\ S_r(h_o, v_r), \text{ if } h_o > h_r. \end{cases} \tag{2.9}$$

Where the left and the right shock waves are

$$S_l(h_o; v_l) = q_o = q_l + (h_o - h_l)\left[\frac{q_l}{h_l} - \sqrt{\frac{g h_o (h_o + h_l)}{2h_l}}\right], \text{ for } h_o > h_l, \tag{2.10}$$

$$S_r(h_o; v_r) = q_o = q_r + (h_o - h_r)\left[\frac{q_r}{h_r} + \sqrt{\frac{g h_o (h_o + h_r)}{2h_r}}\right], \text{ for } h_o > h_r, \tag{2.11}$$

and the left and the right rarefaction waves are

$$R_l(h_o; v_l) = q_o = h_o\left(\frac{q_l}{h_l} + 2\sqrt{g h_l} - 2\sqrt{g h_o}\right), \text{ for } h_o < h_l, \tag{2.12}$$

$$R_r(h_o; v_r) = q_o = h_o \left(\frac{q_r}{h_r} - 2\sqrt{gh_r} + 2\sqrt{gh_o} \right), \text{ for } h_o < h_r. \tag{2.13}$$

Then, the τ_l- curve is

$$\tau_l(h_o; v_l) = \begin{bmatrix} h_o \\ \beta_l(h_o; v_l) \end{bmatrix}, \tag{2.14}$$

and the τ_r- curve is

$$\tau_r(h_o; v_r) = \begin{bmatrix} h_o \\ \beta_r(h_o; v_r) \end{bmatrix}. \tag{2.15}$$

In the next propositions, the extrema of the previous functions are computed to locate the maximum and the minimum of the curve $\tau_l(h_o; v_l)$ and the curve $\tau_r(h_o; v_r)$.

Proposition 2.1. *Considering the sub-critical flow conditions, the only part of the curve $\tau_l(h_o; v_l)$ that can intersect with the positive critical curve C^+ is the rarefaction portion. That intersection, denoted by v_o^{lm}, is characterized by the maximum of β_l and is given by*

$$h_o^{lm} = \frac{1}{g} \left(\frac{q_l}{3h_l} + \frac{2}{3}\sqrt{gh_l} \right)^2, \tag{2.16}$$

$$q_o^{lm} = \beta_l(h_o^{lm}; v_l) = h_o^{lm}\sqrt{gh_o^{lm}}. \tag{2.17}$$

Moreover, $\tau_l(h_o; v_l)$ is given by a concave function that is increasing in the interval $]0, h_o^{lm}]$ and decreasing in the interval $[h_o^{lm}, +\infty[$. Therefore, the increasing part of the function varies from

$$\lim_{h_o \to 0^+} \beta_l(h_o; v_l) = 0 \quad to \quad \beta_l(h_o^{lm}; v_l) = h_o^{lm}\sqrt{gh_o^{lm}}, \tag{2.18}$$

and the decreasing part varies from

$$\beta_l(h_o^{lm}; v_l) = h_o^{lm}\sqrt{gh_o^{lm}} \quad to \lim_{h_o \to +\infty} \beta_l(h_o; v_l) = -\infty. \tag{2.19}$$

Proof. The general idea is summarized as follow: First, assuming that the shock portion is intersected with the critical curve C^+. Then, one can show that this assumption violates the sub-critical flow conditions. Indeed, the proof follows by contradiction, see [24]. □

Proposition 2.2. *Considering the sub-critical flow conditions, the only part of the curve $\tau_r(h_o; v_r)$ that can intersect with the critical curve C^- is the rarefaction portion. That intersection, denotes by v_o^{rm}, is characterized by the minimum of β_r and is given by*

$$h_o^{rm} = \frac{1}{g} \left(-\frac{q_r}{3h_r} + \frac{2}{3}\sqrt{gh_r} \right)^2, \tag{2.20}$$

$$q_o^{rm} = -\beta_r(h_o^{rm}; v_r) = h_o^{rm}\sqrt{gh_o^{rm}}. \tag{2.21}$$

Moreover, $\tau_r(h_o; v_r)$ is given by a convex function that is decreasing in the interval $]0, h_o^{rm}]$ and increasing in the interval $[h_o^{rm}, +\infty[$. Therefore, the decreasing part of the function varies from

$$\lim_{h_o \to 0^+} \beta_r(h_o; v_r) = 0 \quad to \quad \beta_r(h_o^{rm}; v_r) = -h_o^{rm}\sqrt{gh_o^{rm}}, \tag{2.22}$$

and the increasing part varies from

$$\beta_r(h_o^{rm}; v_r) = -h_o^{rm}\sqrt{gh_o^{rm}} \quad to \lim_{h_o \to +\infty} \beta_r(h_o; v_r) = +\infty. \tag{2.23}$$

Proof. Look at the proof of Proposition 2.1. □

We can also prove that the states (h_o, q_o) such that $h_o < h_o^{lm}$ and $h_o < h_o^{rm}$ violate the sub-critical flow conditions. Therefore, Proposition 2.1 and proposition 2.2 assure that $\tau_l(h_o; v_l)$ and $\tau_r(h_o; v_r)$ intersect only at one point which is the intermediate state v_* in the solution of the standard Riemann problem (2.3) and (2.7). Furthermore, the components (h_*, q_*) of the intermediate state $v_* = \tau_l(h_*; v_l) \cap \tau_r(h_*; v_r)$ are computed by solving the following nonlinear function:

$$\beta(h_*; v) \equiv \beta_l(h_*; v_l) - \beta_r(h_*, v_r) = 0. \tag{2.24}$$

Example 2.1. We present the standard Riemann solution of (2.3) and (2.7) with initial data:

$$v_l = \begin{bmatrix} h_l \\ q_l \\ z_l \end{bmatrix} = \begin{bmatrix} 1 \\ 0 \\ 0 \end{bmatrix}, \quad v_r = \begin{bmatrix} h_r \\ q_r \\ z_r \end{bmatrix} = \begin{bmatrix} 0.5 \\ 0 \\ 0 \end{bmatrix}. \tag{2.25}$$

Figure 2 represents the Riemann solution of Example 2.1. In the regions above the curve C^+ and below the curve C^-, the sub-critical flow conditions are not satisfied. Note that these regions are the same in all next figures of Section 3 and Section 4. The dot lines represent the left and right rarefaction ($R_l(h_o; v_l)$ and $R_r(h_o; v_r)$). The solid lines represent the left shock and right shock ($S_l(h_o; v_l)$ and $S_r(h_o; v_r)$). The intermediate state v_* in the Riemann solution is the intersection between the curves τ_l and τ_r. The intermediate state is connected to the left initial state v_l through a rarefaction (dot line) and to the right initial state v_r through a shock (solid line). The state v_o^{lm} is the maximum value of the left- curve τ_l and corresponds to the intersection between the left-curve τ_l and the critical curve C^+. Similarly, the state v_o^{rm} is the minimum of the right curve τ_r and corresponds to the intersection between the right curve τ_r and the critical curve C^-. For more clarification, Figure 3 shows the evolution of the Riemann solution plotted at $t = 0.2[s]$. It is clear that the solution consists of two waves, the first is a rarefaction and the second is a shock, and the intermediate state.

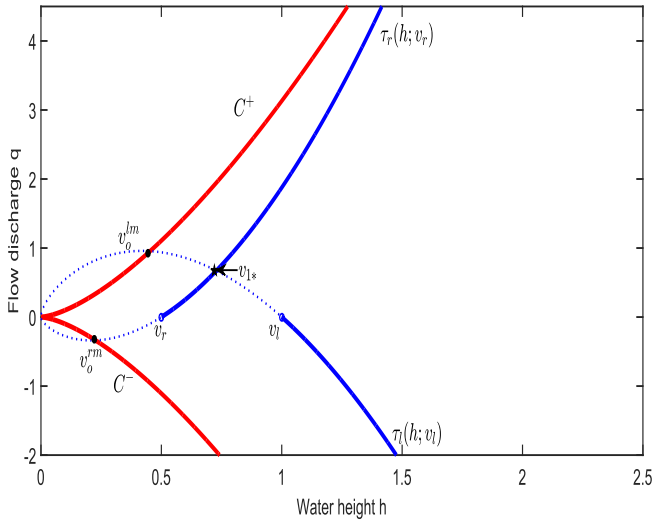

Fig. 2. The solution of the standard Riemann problem in a single channel.

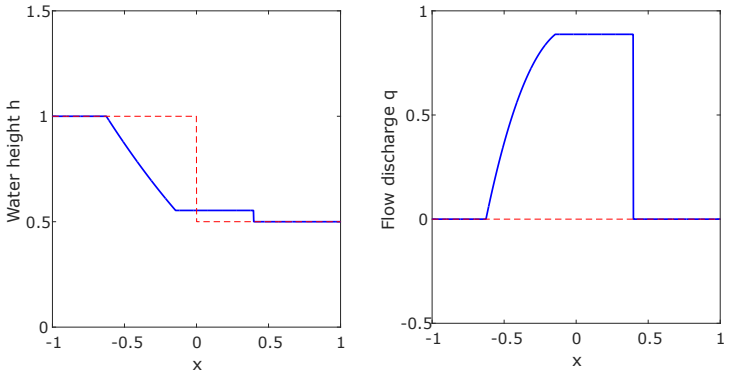

Fig. 3. Water height and flow discharge profiles in the standard Riemann solution at $t = 0.2[s]$, are shown in solid lines. The initial data are shown in dot lines.

3. Nonlinear junction Riemann problem

In this Section, we newly provide the solution structure of the junction Riemann problem in the presence of bottom discontinuities and for non-symmetric downstream channels with possible different channels width. By considering the star

network reported in Fig.1, the shallow water equations are defined as:

$$\begin{cases} \frac{\partial v_1}{\partial t} + A_1(v_1)\frac{\partial v_1}{\partial x} = 0, & x < x_J, \\ \frac{\partial v_2}{\partial t} + A_2(v_2)\frac{\partial v_2}{\partial x} = 0, & x > x_J, \\ \frac{\partial v_3}{\partial t} + A_3(v_3)\frac{\partial v_3}{\partial x} = 0, & x > x_J, \end{cases} \tag{3.1}$$

where x_J is the junction point and $A(v)$ is defined in (2.4). The junction Riemann problem is given and governed by the initial data:

$$\begin{cases} v_1(0,x) = v_{1l}, & x < x_J, \\ v_2(0,x) = v_{2r}, & x > x_J, \\ v_2(0,x) = v_{3r}, & x > x_J. \end{cases} \tag{3.2}$$

Considering the Riemann problem (3.1-3.2), the Riemann solution consists of six states denote by v_{1l}, v_{2r}, v_{3r}, v_{1*}, v_{2*}, and v_{3*}. From v_{1l} to v_{1*}, the relationship (2.10) or (2.12) holds. From v_{2r} to v_{2*} and from v_{3r} to v_{3*}, the relationship (2.11) or (2.13) holds. The states v_{1*}, v_{2*}, and v_{3*} are connected to each other by the mass conservation and the total head balance relationships. The following conditions are obtained

$$q_{1*} = \omega_2 q_{2*} + \omega_3 q_{3*}; \quad q_{2*} = \left(\frac{r}{\omega_2}\right) q_{1*}, \quad q_{3*} = \left(\frac{1-r}{\omega_3}\right) q_{1*}, \quad \text{at } x_J, \tag{3.3}$$

$$h_{1*} + \frac{q_{1*}^2}{2gh_{1*}^2} = Z_2 + h_{2*} + \frac{q_{2*}^2}{2gh_{2*}^2}, \quad \text{at } x_J, \tag{3.4}$$

$$h_{1*} + \frac{q_{1*}^2}{2gh_{1*}^2} = Z_3 + h_{3*} + \frac{q_{3*}^2}{2gh_{3*}^2}, \quad \text{at } x_J, \tag{3.5}$$

where $0 < r = \omega_2 \frac{q_{2*}}{q_{1*}} < 1$ is the discharge ratio. $0 < \omega_2 = \frac{b_2}{b_1}$ and $0 < \omega_3 = \frac{b_3}{b_1}$ are the ratio between the second channel width and the first channel width, and the third channel width and the first channel width, respectively. $Z_2 = z_2 - z_1$ and $Z_3 = z_3 - z_1$ are the bottom discontinuities between the first and the second channels, and between the first and the third channels, respectively. The conditions at the junction ($x_J = 0$) are the conservation of mass and the total head balances. For a more detailed discussion about the physical meaning of the total head concept and its relation to the flow depth ratio, we refer to [30, 31].
Moreover, the correct left wave connecting v_{1*} to v_{1l} is

$$q_{1*} = \beta_{1l}(h_{1*}; v_{1l}), \tag{3.6}$$

where β_{1l} is given by (2.8), and the correct right waves connecting v_{2*} to v_{2r} and v_{3*} to v_{3r} are

$$q_{2*} = \beta_{2r}(h_{2*}; v_{2r}), \tag{3.7}$$

and

$$q_{3*} = \beta_{3r}(h_{3*}; v_{3r}), \tag{3.8}$$

where β_{2r} and β_{3r} are given by (2.9), respectively.

3.1. *Existence and uniqueness of the solution of the nonlinear junction Riemann problem*

In this subsection, we show that the solution of the junction Riemann problem (3.1-3.2) exists under certain hypothesis and is unique under sub-critical flow conditions. Moreover, we demonstrate also the conditions for which the solution does not exist. Hence, we look to find $(h_{1*}, h_{2*}, h_{3*}, q_{1*}, q_{2*}, q_{3*})$ that satisfy (3.3-3.8), while system (3.6-3.8) consists of eight possible combination. These possible combinations are:

(1) If $h_{1*} < h_{1l}$, $h_{2*} < h_{2r}$, and $h_{3*} < h_{3r}$ i.e., left and right waves are rarefaction, then (v_{1*}, v_{2*}, v_{3*}) satisfies (3.3-3.5) such that $v_{1*} \in R_{1l}$, $v_{2*} \in R_{2r}$, and $v_{3*} \in R_{3r}$.
(2) If $h_{1*} > h_{1l}$, $h_{2*} > h_{2r}$, and $h_{3*} > h_{3r}$ i.e., left and right waves are shock, then (v_{1*}, v_{2*}, v_{3*}) satisfies (3.3-3.5) such that $v_{1*} \in S_{1l}$, $v_{2*} \in S_{2r}$, and $v_{3*} \in S_{3r}$.
(3) If $h_{1*} < h_{1l}$, $h_{2*} > h_{2r}$, and $h_{3*} > h_{3r}$ i.e., left rarefaction wave and right shock waves, then (v_{1*}, v_{2*}, v_{3*}) satisfies (3.3-3.5) such that $v_{1*} \in R_{1l}$, $v_{2*} \in S_{2r}$, and $v_{3*} \in S_{3r}$.
(4) If $h_{1*} > h_{1l}$, $h_{2*} < h_{2r}$, and $h_{3*} < h_{3r}$ i.e., left shock wave and right rarefaction waves, then (v_{1*}, v_{2*}, v_{3*}) satisfies (3.3-3.5) such that $v_{1*} \in S_{1l}$, $v_{2*} \in R_{2r}$, and $v_{3*} \in R_{3r}$.
(5) If $h_{1*} > h_{1l}$, $h_{2*} > h_{2r}$, and $h_{3*} < h_{3r}$ i.e., left shock wave, first right shock wave, and second right rarefaction wave, then (v_{1*}, v_{2*}, v_{3*}) satisfies (3.3-3.5) such that $v_{1*} \in S_{1l}$, $v_{2*} \in S_{2r}$, and $v_{3*} \in R_{3r}$.
(6) If $h_{1*} > h_{1l}$, $h_{2*} < h_{2r}$, and $h_{3*} > h_{3r}$ i.e., left shock wave, first right rarefaction wave, and second right shock wave, then (v_{1*}, v_{2*}, v_{3*}) satisfies (3.3-3.5) such that $v_{1*} \in S_{1l}$, $v_{2*} \in R_{2r}$, and $v_{3*} \in S_{3r}$.
(7) If $h_{1*} < h_{1l}$, $h_{2*} > h_{2r}$, and $h_{3*} < h_{3r}$ i.e., left rarefaction wave, first right shock wave, and second right rarefaction wave, then (v_{1*}, v_{2*}, v_{3*}) satisfies (3.3-3.5) such that $v_{1*} \in R_{1l}$, $v_{2*} \in S_{2r}$, and $v_{3*} \in R_{3r}$.
(8) If $h_{1*} < h_{1l}$, $h_{2*} < h_{2r}$, and $h_{3*} > h_{3r}$ i.e., left rarefaction wave, first right rarefaction wave, and second right shock wave, then (v_{1*}, v_{2*}, v_{3*}) satisfies (3.3-3.5) such that $v_{1*} \in R_{1l}$, $v_{2*} \in R_{2r}$, and $v_{3*} \in S_{3r}$.

3.1.1. *Mass-energy conservation at the junction.*

For any left sub-critical state v_{1*}, the states v_{2*} and v_{3*} are computed by solving the junction conditions (3.3-3.5). The states v_{2*} and v_{3*} are sub-critical states with $h_{2*} > 0$ and $h_{3*} > 0$. Substituting the mass equation (3.3) in the total head balances (3.4-3.5), the junction conditions give the following algebraic equations:

$$h_{2*}^3 + a_2 h_{2*}^2 + c_2 = 0,\ a_2 = -h_{1*} + Z_2 - \frac{q_{1*}^2}{2g h_{1*}^2},\ c_2 = \left(\frac{r}{\omega_2}\right)^2 \frac{q_{1*}^2}{2g} \geq 0, \tag{3.9}$$

$$h_{3*}^3 + a_3 h_{3*}^2 + c_3 = 0,\ a_3 = -h_{1*} + Z_3 - \frac{q_{1*}^2}{2g h_{1*}^2},\ c_3 = \left(\frac{1-r}{\omega_3}\right)^2 \frac{q_{1*}^2}{2g} \geq 0. \tag{3.10}$$

The specific energy of each cross section (AB, CD, EF) at the channels junction can be written as follows:

$$E_{1*} = h_{1*} + \frac{q_{1*}^2}{2gh_{1*}^2},\ E_{2*} = h_{1*} + \left(\frac{r}{\omega_2}\right)^2 \frac{q_{1*}^2}{2gh_{2*}^2},\ E_{3*} = h_{1*} + \left(\frac{1-r}{\omega_3}\right)^2 \frac{q_{1*}}{2gh_{3*}^2}. \tag{3.11}$$

The corresponding critical flow depths can be written as:

$$h_{c1} = \sqrt[3]{\frac{q_{1*}^2}{g}},\quad h_{c2} = \sqrt[3]{\left(\frac{r}{\omega_2}\right)^2 \frac{q_{1*}^2}{g}},\quad h_{c3} = \sqrt[3]{\left(\frac{1-r}{\omega_3}\right)^2 \frac{q_{1*}^2}{g}}, \tag{3.12}$$

respectively, being:

$$h_{c2} = \left(\frac{r}{\omega_2}\right)^{\frac{2}{3}} h_{c1},\quad h_{c3} = \left(\frac{1-r}{\omega_3}\right)^{\frac{2}{3}} h_{c1}. \tag{3.13}$$

Using the critical depth h_{c1} as the reference depth, the critical specific energy in each cross section at the junction can be written as:

$$E_{c1} = \frac{3}{2}h_{c1},\quad E_{c2} = \frac{3}{2}\left(\frac{r}{\omega_2}\right)^{\frac{2}{3}} h_{c1},\quad E_{c3} = \frac{3}{2}\left(\frac{1-r}{\omega_3}\right)^{\frac{2}{3}} h_{c1} \tag{3.14}$$

The critical depth h_{c1} and the critical specific energy E_{c1} are used to dimensionless all the depths and all the specific energies in the three channels. The non-dimensional depths are:

$$\eta_1 = \frac{h_{1*}}{h_{c1}},\quad \eta_2 = \frac{h_{2*}}{h_{c1}},\quad \eta_3 = \frac{h_{3*}}{h_{c1}}. \tag{3.15}$$

and the non-dimensional specific energies are:

$$\Gamma_1 = \frac{E_{1*}}{E_{c1}},\quad \Gamma_2 = \frac{E_{2*}}{E_{c1}},\quad \Gamma_3 = \frac{E_{3*}}{E_{c1}}. \tag{3.16}$$

So that the fundamental relations between the non-dimensional specific energy and the non-dimensional depth at each channel are [31]:

$$\Gamma_1 = \frac{2}{3}\eta_1 + \frac{1}{3}\frac{1}{\eta_1^2},\quad \Gamma_2 = \frac{2}{3}\eta_2 + \frac{1}{3}\left(\frac{r}{\omega_2}\right)^2 \frac{1}{\eta_2^2},\quad \Gamma_3 = \frac{2}{3}\eta_3 + \frac{1}{3}\left(\frac{1-r}{\omega_3}\right)^2 \frac{1}{\eta_3^2}. \tag{3.17}$$

The relationships (3.17) are plotted in Fig. 4, for a set of parameters $r = 0.7$, $\omega_2 = 0.2$, and $\omega_3 = 0.8$. In the following, the influence on the solution of r and ω into the solutions is highlighted. The variables η and Γ are investigated in the following domains:

$$1 < \eta_1 < \infty,\quad \left(\frac{r}{\omega_2}\right)^{\frac{2}{3}} < \eta_2 < \infty,\quad \left(\frac{1-r}{\omega_3}\right)^{\frac{2}{3}} < \eta_3 < \infty, \tag{3.18}$$

$$1 \le \Gamma_1 < \infty,\quad \left(\frac{r}{\omega_2}\right)^{\frac{2}{3}} \le \Gamma_2 < \infty,\quad \left(\frac{1-r}{\omega_3}\right)^{\frac{2}{3}} \le \Gamma_3 < \infty. \tag{3.19}$$

Since the study is limited to sub-critical flows, both the choking of the flow and the critical transition are excluded from the present analysis. In other word, the specific

energy in any cross section in the channel is larger than the critical value, that is necessary to cross over the junction. Using (3.15-3.17), then equations (3.9-3.10)

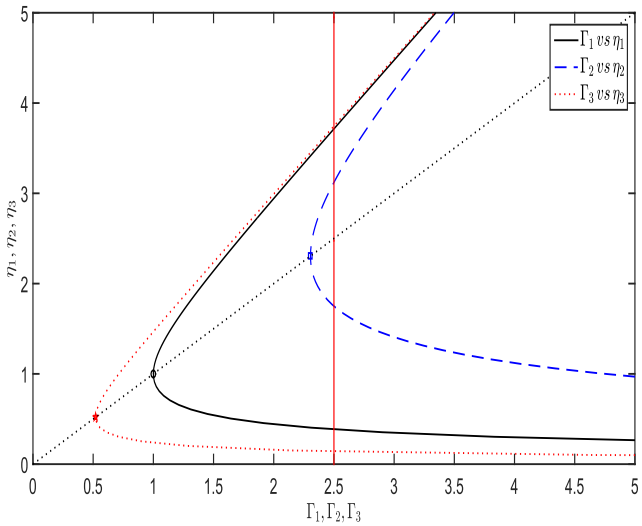

Fig. 4. Energy *vs* depth

are written in the following non-dimensional form

$$\eta_2^3 + \alpha_2\eta_2^2 + \mu_2 = 0,\ \alpha_2 = -\frac{3}{2}\Gamma_1 + \Delta\xi_2,\ \mu_2 = \frac{1}{2}\left(\frac{r}{\omega_2}\right)^2, \tag{3.20}$$

$$\eta_3^3 + \alpha_3\eta_3^2 + \mu_3 = 0,\ \alpha_3 = -\frac{3}{2}\Gamma_1 + \Delta\xi_3,\ \mu_3 = \frac{1}{2}\left(\frac{1-r}{\omega_3}\right)^2, \tag{3.21}$$

where $\Delta\xi_2 = \frac{Z_2}{h_{c1}}$ and $\Delta\xi_3 = \frac{Z_3}{h_{c1}}$ are the non-dimensional bottom discontinuities. Eq. (3.20) and Eq. (3.21) are based on the use of the following third degree polynomial:

$$P(\eta) = \eta^3 + \alpha\eta^2 + \mu; \quad \eta = (\eta_2, \eta_3) \quad \alpha = (\alpha_2, \alpha_3), \quad \mu = (\mu_3, \mu_3). \tag{3.22}$$

Considering the proper domains of r and ω, then μ is always positive. For the forward facing step bottom the maximum permitted height of step is simply equal to the difference between the upstream specific energy and the critical downstream specific energy [30], that is:

$$\frac{2}{3}\Delta\xi_2 \le \Gamma_1 - \left(\frac{r}{\omega_2}\right)^{\frac{2}{3}}, \quad \frac{2}{3}\Delta\xi_3 \le \Gamma_1 - \left(\frac{1-r}{\omega_3}\right)^{\frac{2}{3}}. \tag{3.23}$$

It is worth nothing that (3.23) and the restriction to sub-critical conditions imply $\alpha < 0$, while $\mu > 0$ comes from the constrains on r.

Using Cardano's method [33], the roots of Eq. (3.22) are shown to be dependent on the following discriminants:

$$\Delta_2 = \mu_2 \left(\frac{4}{27}\alpha_2^3 + \mu_2 \right), \tag{3.24}$$

$$\Delta_3 = \mu_3 \left(\frac{4}{27}\alpha_3^3 + \mu_3 \right). \tag{3.25}$$

$\Delta > 0$ implies complex roots; $\Delta = 0$ implies multiple roots; $\Delta < 0$ implies real roots.

Taking into account the definitions of α and μ in (3.20-3.21) and of sub-critical conditions, the following relations hold:

$$\frac{4}{27}\alpha_2^3 + \mu_2 = -\frac{1}{2}\left(\Gamma_1 - \frac{2}{3}\Delta\xi_2\right)^3 + \frac{1}{2}\left(\frac{r}{\omega_2}\right)^2 = -\frac{1}{2}\Gamma_2^3 + \frac{1}{2}\left(\frac{r}{\omega_2}\right)^2 < 0, \tag{3.26}$$

$$\frac{4}{27}\alpha_3^3 + \mu_3 = -\frac{1}{2}\left(\Gamma_1 - \frac{2}{3}\Delta\xi_3\right)^3 + \frac{1}{2}\left(\frac{1-r}{\omega_3}\right)^2 = -\frac{1}{2}\Gamma_3^3 + \frac{1}{2}\left(\frac{1-r}{\omega_3}\right)^2 < 0 \tag{3.27}$$

in the physical domain of Γ_1, Γ_2, and Γ_3 in (3.19).

Considering $\mu > 0$ and Equations (3.26-3.27), then $\Delta < 0$ and therefore the polynomial (3.22) has three real roots. Equation (3.23) is equivalent to $\Delta_2 < 0$ and $\Delta_3 < 0$, therefore the restriction on the discriminants is related to the step height compared with the specific energy values.

For a given set (Γ_1, $\Delta\xi_2$, $\Delta\xi_3$), the admissible range of $\frac{r}{\omega_2}$ and of $\frac{1-r}{\omega_3}$ can be obtained:

$$\left(\frac{r}{\omega_2}\right) \leq \left(\Gamma_1 - \frac{2}{3}\Delta\xi_2\right)^{\frac{3}{2}}, \quad \left(\frac{1-r}{\omega_3}\right) \leq \left(\Gamma_1 - \frac{2}{3}\Delta\xi_3\right)^{\frac{3}{2}}. \tag{3.28}$$

The discharge ratio r and the width ratio ω, as defined in equation (3.3), have to satisfy conditions (3.28) for a certain set of η_1 and $\Delta\xi$. Conditions (3.28) can be read as the maximum degree of the channels width contraction that is compatible with the flow across the junction.

Considering the following expressions:

$$-1 - \frac{27\alpha_2}{2\mu_2^3} = -1 + 2\left(\frac{r}{\omega_2}\right)^2 \frac{1}{\Gamma_2^3}, \quad -1 - \frac{27\alpha_3}{2\mu_3^3} = -1 + 2\left(\frac{1-r}{\omega_3}\right)^2 \frac{1}{\Gamma_3^3}, \tag{3.29}$$

and using the physical domains defined in Eq. (3.19), it is :

$$-1 < -1 - \frac{27\alpha}{2\mu^3} < 1, \quad 0 < \theta = \arccos\left(-1 - \frac{27\alpha}{2\mu^3}\right) < \pi. \tag{3.30}$$

Taking into account that $\Delta < 0$ and the inequalities in Eq. (3.30), then using Cardano's method and trigonometry properties, the polynomial (3.22) has three real roots. The first root is

$$\eta^{(1)} = \left(\frac{1}{2}\Gamma_1 - \frac{1}{3}\Delta\xi\right)\left[1 - 2\cos\left(\frac{\theta}{3}\right)\right]. \tag{3.31}$$

From (3.19) and (3.30), $\eta^{(1)}$ is shown to be real and negative and therefore is excluded. The second root is

$$\eta^{(2)} = \left(\frac{1}{2}\Gamma_1 - \frac{1}{3}\Delta\xi\right)\left[1 - 2\cos\left(\frac{2\pi - \theta}{3}\right)\right]. \tag{3.32}$$

From (3.19) and (3.30), $\eta^{(2)}$ is shown to be positive and less than $\left(\frac{r}{\omega_2}\right)^{2/3}$ for the second channel and less than $\left(\frac{1-r}{\omega_3}\right)^{2/3}$ for the third channel. The root $\eta^{(2)}$ is the super-critical solution and therefore is excluded from the next analysis. The third root is

$$\eta^{(3)} = \left(\frac{1}{2}\Gamma_1 - \frac{1}{3}\Delta\xi\right)\left[1 - 2\cos\left(\frac{2\pi + \theta}{3}\right)\right]. \tag{3.33}$$

From (3.19) and (3.30), $\eta^{(3)}$ is shown to be real and positive. It is greater than $\left(\frac{r}{\omega_2}\right)^{2/3}$ for the second channel and greater than $\left(\frac{1-r}{\omega_3}\right)^{2/3}$ for the third channel. The root $\eta^{(3)}$ is the sub-critical solution. The following Proposition summarize the previous results in terms of dimensional variables with $Y = \eta^{(3)} h_{c1}$ and $\eta^{(3)} = (\eta_2, \eta_3)$

Proposition 3.1. *For a given left state v_{1*} that satisfies sub-critical flow condition, there are only two right states v_{2*} and v_{3*} that satisfy the junction conditions (3.3-3.5). The right states are*

$$v_{2*} = \begin{bmatrix} Y(a_2, c_2) \\ \left(\frac{r}{\omega_2}\right) q_{1*} \\ z_2 \end{bmatrix}; \; Y(a_2, c_2) = -\frac{a_2}{3}\left[1 - 2\cos\left(\frac{2\pi + \theta_2}{3}\right)\right], \tag{3.34}$$

and

$$v_{3*} = \begin{bmatrix} Y(a_3, c_3) \\ \left(\frac{1-r}{\omega_3}\right) q_{1*} \\ z_3 \end{bmatrix}; \; Y(a_3, c_3) = -\frac{a_3}{3}\left[1 - 2\cos\left(\frac{2\pi + \theta_3}{3}\right)\right], \tag{3.35}$$

with

$$a_2 = -h_{1*} + Z_2 - \frac{q_{1*}^2}{2gh_{1*}^2}, \; c_2 = \left(\frac{r}{\omega_2}\right)^2 \frac{q_{1*}^2}{2g}, \; \theta_2 = \arccos\left(-1 - \frac{27c_2}{2a_2^3}\right), \tag{3.36}$$

and

$$a_3 = -h_{1*} + Z_3 - \frac{q_{1*}^2}{2gh_{1*}^2}, \; c_3 = \left(\frac{1-r}{\omega_3}\right)^2 \frac{q_{1*}^2}{2g}, \; \theta_3 = \arccos\left(-1 - \frac{27c_3}{2a_3^3}\right). \tag{3.37}$$

r and ω satisfy (3.28) and (3.3).

3.1.2. *Junction curves.*

Using Sec. 2.3 and Sec. 3.1.1: Let $v_{1o} \in \tau_{1l}(h_{1o}; v_{1l})$, $v_{2o} \in \tau_{2r}(h_{2o}; v_{2r})$, and $v_{3o} \in \tau_{3r}(h_{3o}; v_{3r})$. For any value of h_{1o}, we have $(h_{2\triangleright}, q_{2\triangleright})$ and $(h_{3\triangleright}, q_{3\triangleright})$ the physically admissible states satisfying sub-critical flow conditions that connect to v_{1o} by the junction conditions. Where, the states $(h_{2\triangleright}, q_{2\triangleright})$ and $(h_{3\triangleright}, q_{3\triangleright})$ satisfy

$$h_{2\triangleright} = Y(a_2(h_{1o}), c_2(h_{1o})), \quad q_{2\triangleright} = \frac{r}{\omega_2}\beta_{1l}(h_{1o}; v_{1l}), \tag{3.38}$$

$$h_{3\triangleright} = Y(a_3(h_{1o}), c_3(h_{1o})), \quad q_{3\triangleright} = \frac{(1-r)}{\omega_3}\beta_{1l}(h_{1o}; v_{1l}), \tag{3.39}$$

where $Y(.,.)$ is given by (3.34-3.35) and

$$a_2(h_{1o}) = -h_{1o} + Z_2 - \frac{\beta_{1l}^2(h_{1o}, v_{1l})}{2gh_{1o}^2}, \quad c_2(h_{1o}) = \left(\frac{r}{\omega_2}\right)\frac{\beta_{1l}^2(h_{1o}; v_{1l})}{2g}, \tag{3.40}$$

$$a_3(h_{1o}) = -h_{1o} + Z_3 - \frac{\beta_{1l}^2(h_{1o}; v_{1l})}{2gh_{1o}^2}, \quad c_2(h_{1o}) = \left(\frac{(1-r)}{\omega_3}\right)\frac{\beta_{1l}^2(h_{1o}; v_{1l})}{2g}. \tag{3.41}$$

$\beta_{1l}(h_{1o}, v_{1l})$ is defined by (2.8). Therefore, the junction curves denoted by $J_1(h_{1o}; v_{1l})$ and $J_2(h_{1o}; v_{1l})$ can be defined as follow

$$J_1(h_{1o}; v_{1l}) = \begin{bmatrix} h_{2\triangleright} \\ q_{2\triangleright} \end{bmatrix}, \quad J_2(h_{1o}; v_{1l}) = \begin{bmatrix} h_{3\triangleright} \\ q_{3\triangleright} \end{bmatrix}. \tag{3.42}$$

Note that the intermediate states in the solution of the junction Riemann problem are computed by the intersections of J_1 with τ_{2r} and J_2 with τ_{3r} and their corresponding states on τ_{1l}. The next Propositions describe the extrema of the functions $Y(a_2(h_{1o}, c_2(h_{1o}))$ and $Y(a_3(h_{1o}, c_3(h_{1o}))$.

Proposition 3.2. *The functions $Y(a(h_{1o}), c(h_{1o}))$ are defined in (3.34) and (3.35). They have their minimums at the maximum h_{1o}^{lm} which is given in Proposition 2.1, such that*

$$\begin{cases} \frac{dY(a_2(h_{1o}), c_2(h_{1o}))}{dh_{1o}}|_{h_{1o}=h_{1o}^{lm}} = 0, \\ \frac{d^2Y(a_2(h_{1o}), c_2(h_{1o}))}{dh_{1o}^2}|_{h_{1o}=h_{1o}^{lm}} > 0. \end{cases} \tag{3.43}$$

$$\begin{cases} \frac{dY(a_3(h_{1o}), c_3(h_{1o}))}{dh_{1o}}|_{h_{1o}=h_{1o}^{lm}} = 0, \\ \frac{d^2Y(a_3(h_{1o}), c_3(h_{1o}))}{dh_{1o}^2}|_{h_{1o}=h_{1o}^{lm}} > 0. \end{cases} \tag{3.44}$$

Moreover, the functions $Y(a(h_{1o}, c(h_{1o}))$ are decreasing in $]0, h_{1o}^{lm}]$ and increasing in $[h_{1o}^{lm}, \infty[$. The decreasing part of the functions varies from

$$\lim_{h_{1o}\to 0^+} Y(a_2(h_{1o}), c_2(h_{1o})) = \frac{9}{2}h_{1o}^{lm} - Z_2 \quad \textit{to} \quad Y_{1o}^{lm}, \tag{3.45}$$

$$\lim_{h_{1o}\to 0^+} Y(a_3(h_{1o}), c_3(h_{1o})) = \frac{9}{2}h_{1o}^{lm} - Z_3 \quad \textit{to} \quad Y_{2o}^{lm}. \tag{3.46}$$

while, the increasing part from

$$Y_{1o}^{lm} \quad to \quad \lim_{h_{1o}\to 0^+} Y(a_2(h_{1o}), c_2(h_{1o})) = +\infty, \tag{3.47}$$

$$Y_{2o}^{lm} \quad to \quad \lim_{h_{1o}\to 0^+} Y(a_3(h_{1o}), c_3(h_{1o})) = +\infty, \tag{3.48}$$

with

$$Y_{1o}^{lm} = \left(\frac{h_{1o}^{lm}}{2} - \frac{Z_2}{3}\right)\left[1 - 2\cos\left(\frac{\theta_2 + 2\pi}{3}\right)\right], \tag{3.49}$$

$$Y_{2o}^{lm} = \left(\frac{h_{1o}^{lm}}{2} - \frac{Z_3}{3}\right)\left[1 - 2\cos\left(\frac{\theta_3 + 2\pi}{3}\right)\right], \tag{3.50}$$

such that

$$\theta_2 = \arccos\left(-1 + 2\left(\frac{r}{\omega_2}\right)^2\left(\frac{h_{1o}^{lm}}{h_{1o}^{lm} - \frac{2}{3}\Delta\xi_2}\right)^3\right), \tag{3.51}$$

$$\theta_3 = \arccos\left(-1 + 2\left(\frac{1-r}{\omega_3}\right)^2\left(\frac{h_{1o}^{lm}}{h_{1o}^{lm} - \frac{2}{3}\Delta\xi_3}\right)^3\right). \tag{3.52}$$

Proposition 3.3. *The junction curves $J_1(h_{1o}, v_{1l})$ and $J_2(h_{1o}; v_{1l})$ consist of two branches connected by the minimum states, are denoted by $v_{2\triangleright}^{lm}$ and $v_{3\triangleright}^{lm}$, respectively. These states correspond to v_{1o}^{lm} by the junction conditions, with*

$$\begin{cases} h_{2\triangleright}^{lm} = Y_{1o}^{lm}, \quad q_{2\triangleright}^{lm} = \left(\frac{r}{\omega_2}\right) q_{1o}^{lm}, \\ h_{3\triangleright}^{lm} = Y_{2o}^{lm}, \quad q_{3\triangleright}^{lm} = \left(\frac{1-r}{\omega_3}\right) q_{1o}^{lm}, \end{cases} \tag{3.53}$$

where Y_{1o}^{lm} and Y_{2o}^{lm} are given by Proposition 3.2. q_{1o}^{lm} is given by Proposition 2.1. For any state $(h_{2\triangleright}, q_{2\triangleright})$ on the junction curve $J_1(h_{1o}; v_{1l})$ and $(h_{3\triangleright}, q_{3\triangleright})$ on the junction curve $J_2(h_{1o}; v_{1l})$, we have

$$\begin{cases} h_{2\triangleright} \geq Y_{1o}^{lm}, \\ h_{3\triangleright} \geq Y_{2o}^{lm}. \end{cases} \tag{3.54}$$

Furthermore, the following relations hold

$$\begin{cases} \frac{dh_{2\triangleright}}{dh_{1o}} < 0, \quad \frac{dq_{2\triangleright}}{dh_{1o}} > 0, \quad if\ 0 < h_{1o} < h_{1o}^{lm}, \\ \frac{dh_{3\triangleright}}{dh_{1o}} < 0, \quad \frac{dq_{3\triangleright}}{dh_{1o}} > 0, \quad if\ 0 < h_{1o} < h_{1o}^{lm}, \end{cases} \tag{3.55}$$

$$\begin{cases} \frac{dh_{2\triangleright}}{dh_{1o}} = 0, \quad \frac{dq_{2\triangleright}}{dh_{1o}} = 0, \quad if\ h_{1o} = h_{1o}^{lm}, \\ \frac{dh_{3\triangleright}}{dh_{1o}} = 0, \quad \frac{dq_{3\triangleright}}{dh_{1o}} = 0, \quad if\ h_{1o} = h_{1o}^{lm}, \end{cases} \tag{3.56}$$

$$\begin{cases} \frac{dh_{2\triangleright}}{dh_{1o}} > 0, \quad \frac{dq_{2\triangleright}}{dh_{1o}} < 0, \quad if\ h_{1o}^{lm} < h_{1o} < +\infty, \\ \frac{dh_{3\triangleright}}{dh_{1o}} > 0, \quad \frac{dq_{3\triangleright}}{dh_{1o}} < 0, \quad if\ h_{1o}^{lm} < h_{1o} < +\infty. \end{cases} \tag{3.57}$$

Proposition 3.3 shows that each junction curve has two branches. One branch corresponds to non sub-critical states which satisfies (3.55) and (3.56), and are denoted by $J_{1+}(h_{1o}; v_{1l})$ and $J_{2+}(h_{1o}; v_{1l})$, respectively. This branch is excluded from the analysis for violating sub-critical flow conditions. The second branch of the junction curves, are denoted by $J_{1-}(h_{1o}; v_{1l})$ and $J_{2-}(h_{1o}; v_{2l})$, satisfy (3.56) and (3.57), and corresponds to sub-critical flow conditions. The intermediate states in the solution of the junction Riemann problem are obtained by the intersection of the junction branches J_{1-} and J_{2-}, and the right curves $\tau_{2r}(h_{1o}; v_{2r})$ and $\tau_{3r}(h_{1o}; v_{3r})$, respectively.
Moreover, by considering Propositions 2.1, 2.2, 3.1, 3.2, and 3.3 the solution of the junction Riemann problem is summarized in the following Theorem:

Theorem 3.4. *The Riemann Problem defined in (3.1-3.5) has a unique solution if and only if*

$$\begin{cases} q_{2\triangleright}^{lm} > \beta_{2r}(h_{2\triangleright}^{lm}; v_{2r}), \\ q_{3\triangleright}^{lm} > \beta_{3r}(h_{3\triangleright}^{lm}; v_{3r}), \end{cases} \tag{3.58}$$

where $(h_{2\triangleright}^{lm}, q_{2\triangleright}^{lm})$ and $(h_{3\triangleright}^{lm}, q_{3\triangleright}^{lm})$ are given in Proposition 3.3, and β_{2r} and β_{3r} are given by (2.9), and condition (3.23) is satisfied. Then, the intermediate states in the junction Riemann solution are given by

$$v_{1*} = \begin{bmatrix} h_{1*} \\ q_{1*} \\ z_1 \end{bmatrix} = \begin{bmatrix} h_{1\triangleright} \\ \beta_{1l}(h_{1\triangleright}; v_{1l}) \\ z_1 \end{bmatrix}, \tag{3.59}$$

$$v_{2*} = \begin{bmatrix} h_{2*} \\ q_{2*} \\ z_2 \end{bmatrix} = \begin{bmatrix} Y(a_2(h_{1\triangleright}), c_2(h_{1\triangleright})) \\ \beta_{2r}(Y(a_2(h_{1\triangleright}), c_2(h_{1\triangleright})); v_{2r}) \\ z_2 \end{bmatrix}, \tag{3.60}$$

$$v_{3*} = \begin{bmatrix} h_{3*} \\ q_{3*} \\ z_3 \end{bmatrix} = \begin{bmatrix} Y(a_3(h_{1\triangleright}), c_3(h_{1\triangleright})) \\ \beta_{3r}(Y^{(1)}(a_3(h_{1\triangleright}), c_3(h_{1\triangleright})); v_{3r}) \\ z_3 \end{bmatrix}, \tag{3.61}$$

where $h_{1\triangleright}$ is the solution of

$$\beta(h_{1\triangleright}; v) \equiv \beta_{2r}\left(Y(a_2(h_{1\triangleright}), c_2(h_{1\triangleright})); v_{2r}\right) + \beta_{3r}\left(Y(a_3(h_{1\triangleright}), c_3(h_{1\triangleright})); v_{3r}\right) - \left(\frac{r}{\omega_2} + \frac{1-r}{\omega_3}\right) \beta_{1l}(h_{1\triangleright}; v_{1l}),\ h_{1\triangleright} > h_{1o}^{lm}, \tag{3.62}$$

with h_{1o}^{lm} is given by Eq. (2.16).

Proof. The proof of Theorem 3.4 is summarized as follow: the only valid junction branches that gives sub-critical states are J_{1-} and J_{2-} under the conditions (3.58) and (3.23). This means that the state $q_{2\triangleright}^{lm}$ and $q_{3\triangleright}^{lm}$ are located above the right curves τ_{2r} and τ_{3r}, respectively. Thus, from Proposition 2.1 and Proposition 3.3 it follows

that J_{1-} and J_{2-} intersect at a single point with τ_{2r} and τ_{3r}, respectively. This intersection gives the intermediate states v_{2*} and v_{3*} of the Riemann solution. The intermediate states satisfy the following relationships:

$$h_{2*} = Y(a_2(h_{1\triangleright}), c_2(h_{1\triangleright})); \quad \beta_{2r}(h_{2*}; v_{2r}) = \left(\frac{r}{\omega_2}\right)\beta_{1l}(h_{1\triangleright}; v_{1l}), \tag{3.63}$$

$$h_{3*} = Y(a_3(h_{1\triangleright}), c_3(h_{1\triangleright})); \quad \beta_{3r}(h_{3*}; v_{3r}) = \left(\frac{1-r}{\omega_3}\right)\beta_{1l}(h_{1\triangleright}; v_{1l}). \tag{3.64}$$

Then, for $h_{1\triangleright} > h_{1o}^{lm}$ and combining equation (3.63) and equation (3.64), we get

$$\beta_{2r}\left(Y(a_2(h_{1\triangleright}), c_2(h_{1\triangleright})); v_{2r}\right) + \beta_{3r}\left(Y(a_3(h_{1\triangleright}), c_3(h_{1\triangleright})); v_{3r}\right) - \left(\frac{r}{\omega_2} + \frac{1-r}{\omega_3}\right)\beta_{1l}(h_{1\triangleright}; v_{1l}) = 0,\ h_{1\triangleright} > h_{1o}^{lm}. \tag{3.65}$$

Therefore, the value of $h_{1\triangleright}$ is obtained by finding the root of the following function

$$\beta(h_{1\triangleright}; v) \equiv \beta_{2r}\left(Y(a_2(h_{1\triangleright}), c_2(h_{1\triangleright})); v_{2r}\right) + \beta_{3r}\left(Y(a_3(h_{1\triangleright}), c_3(h_{1\triangleright})); v_{3r}\right) - \left(\frac{r}{\omega_2} + \frac{1-r}{\omega_3}\right)\beta_{1l}(h_{1\triangleright}; v_{1l}),\ h_{1\triangleright} > h_{1o}^{lm}. \tag{3.66}$$

Moreover, the intermediate state v_{1*} in the Riemann solution is

$$v_{1*} = \begin{bmatrix} h_{1*} \\ q_{1*} \\ z_1 \end{bmatrix} = \begin{bmatrix} h_{1\triangleright} \\ \beta_{1l}(h_{1\triangleright}; v_{1l}) \\ z_1 \end{bmatrix}. \tag{3.67}$$

On the other side, the curves J_{1-}, J_{2-} and τ_{2r}, τ_{3r} intersect only if $v_{2\triangleright}^{lm}$ is above the curve τ_{2r} and $v_{3\triangleright}^{lm}$ above the curve τ_{3r}. Therefore, if $v_{2\triangleright}^{lm} \in \tau_{2r}$ and $v_{3\triangleright}^{lm} \in \tau_{3r}$, the intermediate states are given by $(v_{1o}^{lm}, v_{2\triangleright}^{lm})$ and $(v_{1o}^{lm}, v_{3\triangleright}^{lm})$, are not valid states because Proposition 2.1 shows that v_{1o}^{lm} is a critical state. Then, condition (3.58) holds and condition (3.23) must be satisfied, to avoid complex roots. Indeed, the proof of the theorem is completed. □

4. Numerical examples

In this section some examples of the solutions of the nonlinear junction Riemann problem are presented. The solutions are plotted in two phases. The first phase is the $h-q$ phase plane. The second phase is the $h-x$ and $q-x$ phase planes at a fixed time. Both symmetric case (i.e., the two downstream channels are symmetric) without bottom discontinuities, and the non-symmetric case with bottom discontinuities and different channels width, are presented. The behavior of the different solutions is investigated. To supply r, the nonlinear system (3.3-3.8) is numerically solved by using a hybrid method for nonlinear equations [34]. This implies that r is computable if the system (3.3-3.8) admits a numerical solution and therefore the computed value of r is considered. For the case in which the system (3.3-3.8) does not admit a numerical solution, r is chosen for a purpose of declaration.

Example 4.1. We consider the following initial Riemann data

$$v_{1l} = \begin{bmatrix} 1.1 \\ 1.2 \\ 0 \end{bmatrix}, \quad v_{2r} = \begin{bmatrix} 1.2 \\ 0.3 \\ 0 \end{bmatrix}, \quad v_{3r} = \begin{bmatrix} 1.2 \\ 0.3 \\ 0 \end{bmatrix} \tag{4.1}$$

for the symmetric case of the downstream flow (i.e., $b_1 = b_2 = b_3$ and $r = 0.5$) by the symmetry of the downstream flow.

Figure 5 shows that the solution in the three channels consists of three intermediate

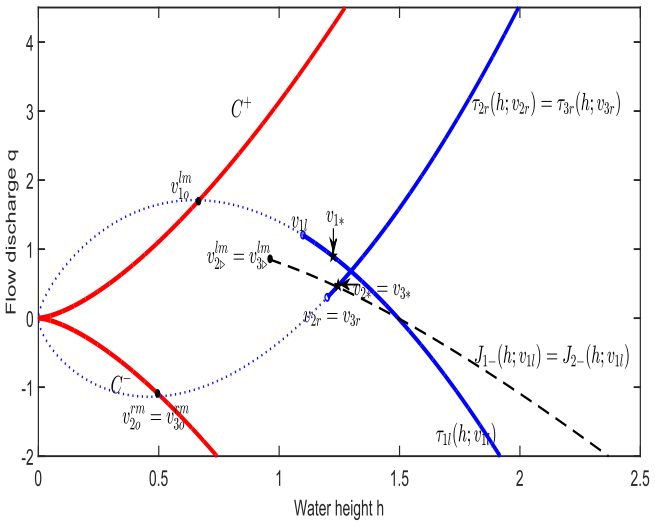

Fig. 5. The solution of the junction Riemann problem in symmetric case and without bottom discontinuities.

states. The intermediate states are v_{1*}, v_{2*} , and v_{3*}. The states v_{2*} and v_{3*} are coincident due to the symmetry of the downstream flow. The intermediate states $v_{2*} = v_{3*}$ are obtained by the intersection of the junction curve J_- (dash line), and the right wave curves τ_{2r} and τ_{3r} (dot-solid line). The state v_{1*} is the corresponding state, and belongs to the left wave curve τ_{1l}. Then, the solution is completed by a left shock (solid line) that connects the states v_{1l} and v_{1*} in the first channel. The states $v_{2r} = v_{3r}$ are connected to the states $v_{2*} = v_{3*}$ through a shock (solid line) for the second and the third channels. Indeed, condition (3.58) is satisfied. Figure 6 shows the evolution of water height and flow discharges profiles in the three channels at $t = 0.2\,[s]$. The junction Riemann solution is represented by solid lines and the dash lines represent the initial data profile. The intermediate states in the Riemann solution satisfy the mass-energy conservation at the junction. The solution consists of a shock occurring in the first channel for $x < 0$, a shock occurring in the second channel for $x > 0$, and a shock occurring in the third channel for $x > 0$.

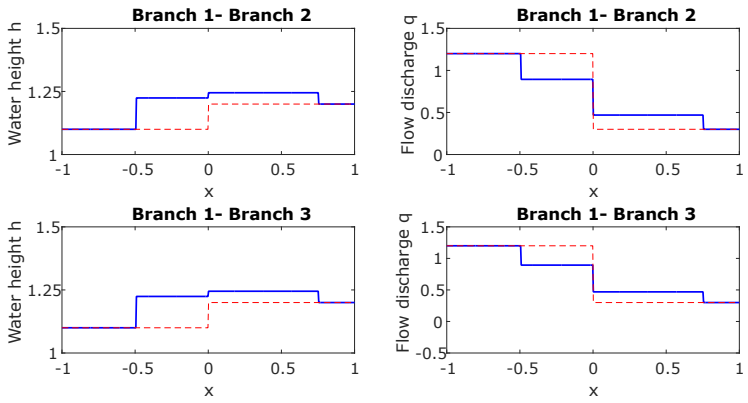

Fig. 6. Water height and flow discharge evolution of junction Riemann solution in symmetric case and without bottom discontinuities at $t = 0.2[s]$.

In the next examples, we demonstrate the effect of the backward bottom discontinuities on the Riemann solution.

Example 4.2. We consider the following initial data with small backward bottom discontinuities $z_1 > (z_2, z_3)$ and the computed $r = 0.76$. The widths $b_1 = 1, b_2 = 0.9$, and $b_3 = 0.5$ are considered.

$$v_{1l} = \begin{bmatrix} 1.1 \\ 1.2 \\ 0.1 \end{bmatrix}, \quad v_{2r} = \begin{bmatrix} 1.2 \\ 0.3 \\ 0 \end{bmatrix}, \quad v_{3r} = \begin{bmatrix} 1.3 \\ 0.3 \\ 0 \end{bmatrix}. \tag{4.2}$$

The junction Riemann solution is shown in Fig. 7 for small backward bottom discontinuities. The junction curves are shown by dash lines that intersect with the wave curves (dot-solid lines) and therefore the intermediate states in the Riemann solution are obtained. The intermediate states v_{1*}, v_{2*}, and v_{3*} are connected to the initial states v_{1l}, v_{2r}, and v_{3r} though a left shock (solid-line) for the first channel, a right shock (solid-line) for the second channel, and a right shock (solid-line) for the third channel, respectively. The Riemann solution exists and therefore (3.67) and (3.23) are satisfied. In Fig. 8, the evolution of water height and flow discharge at time $t = 0.2\,[s]$ are plotted. The Riemann solution is shown by the solid lines and the initial data are in dash lines. The solution consists of a shock occurring in the first channel for $x < 0$, a shock occurring in the second channel for $x > 0$, and a shock occurring in the third channel for $x > 0$. Mass and energy are conserved by the intermediate states while r and ω satisfy condition (3.23).

Example 4.3. Consider the following initial data with large backward bottom discontinuities with $r = 0.75$. The widths $b_1 = 1$, $b_2 = 0.9$, and $b_3 = 0.5$ are

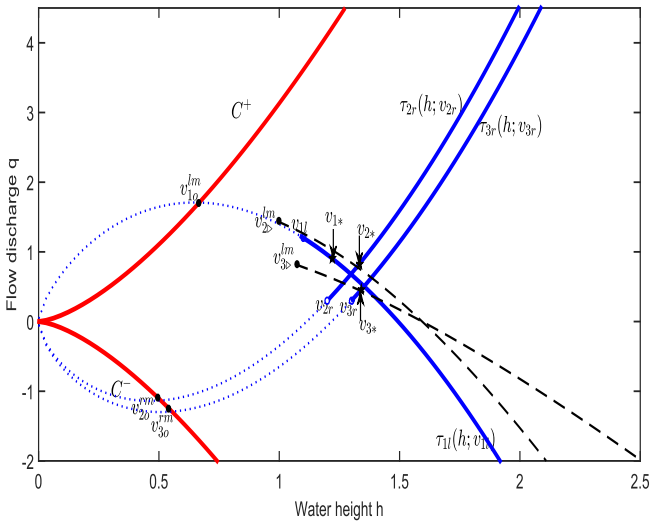

Fig. 7. The solution of the junction Riemann problem with small backward bottom discontinuities (e.g., $z_1 = 0.1$, $z_2 = z_3 = 0$) and with the computed $r = 0.76$.

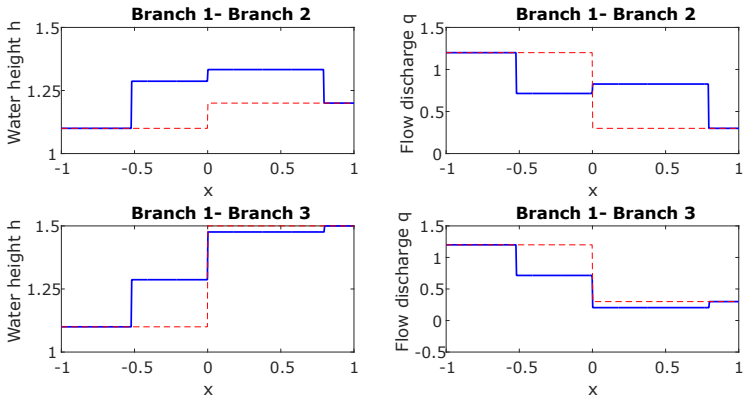

Fig. 8. Water height and flow discharge evolution for junction Riemann solution in non symmetric case and with small backward bottom discontinuities at $t = 0.2[s]$.

considered.

$$v_{1l} = \begin{bmatrix} 1.1 \\ 1.2 \\ 0.8 \end{bmatrix}, \quad v_{2r} = \begin{bmatrix} 1.2 \\ 0.3 \\ 0.0 \end{bmatrix}, \quad v_{3r} = \begin{bmatrix} 1.3 \\ 0.3 \\ 0.0 \end{bmatrix}. \tag{4.3}$$

Figure 9 shows that the Riemann solution does not exist while condition (3.67) is violated and there is not an intersection between the junction curves and the right

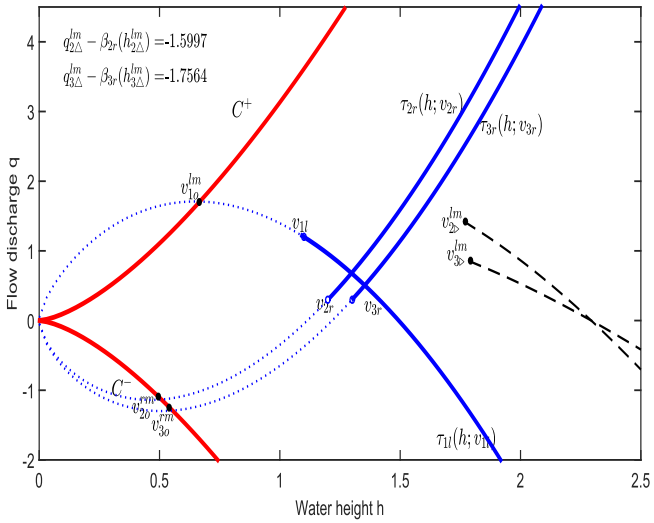

Fig. 9. The solution of the junction Riemann problem with large backward bottom discontinuous (e.g., $z_1 = 0.8$, $z_2 = z_3 = 0$) and $r = 0.75$.

wave curves. Here, the backward bottom step minimize the existence of the Riemann solution. This might be due to energy dissipation and considering an energy correction may extend the existence field of the solution.

In the next examples, we demonstrate the effect of the forward bottom discontinuities on the Riemann solution.

Example 4.4. We consider the following initial data with small forward bottom discontinuities $(z_2, z_3) > z_1$ with the computed $r = 0.75$. The widths $b_1 = 1$, $b_2 = 0.9$, and $b_3 = 0.5$ are considered.

$$v_{1l} = \begin{bmatrix} 1.1 \\ 1.2 \\ 0.0 \end{bmatrix}, \quad v_{2r} = \begin{bmatrix} 1.2 \\ 0.3 \\ 0.1 \end{bmatrix}, \quad v_{3r} = \begin{bmatrix} 1.3 \\ 0.3 \\ 0.1 \end{bmatrix}. \tag{4.4}$$

Figure 10 shows that the Riemann solution exists under small forward bottom discontinuities. The solution consists of a shock that connects the left initial state to the first intermediate state in the first channel. The right initial state is connected to the second intermediate state by a shock in the second channel. For the third channel, a rarefaction connects the second right initial state and the third intermediate state. The three intermediate states are connected by the junction relationships. r and ω satisfy condition (3.23). Conditions (3.67) and (3.23) are satisfied. The evolution of the solution at $t = 0.2\,[s]$ is shown in Fig. 11.

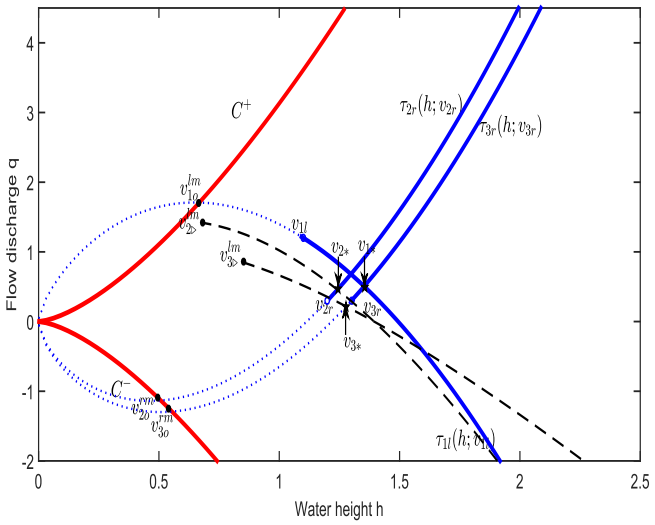

Fig. 10. The solution of the junction Riemann problem with small forward bottom discontinuities (e.g., $z_1 = 0.0$, $z_2 = z_3 = 0.1$) and the computed $r = 0.75$.

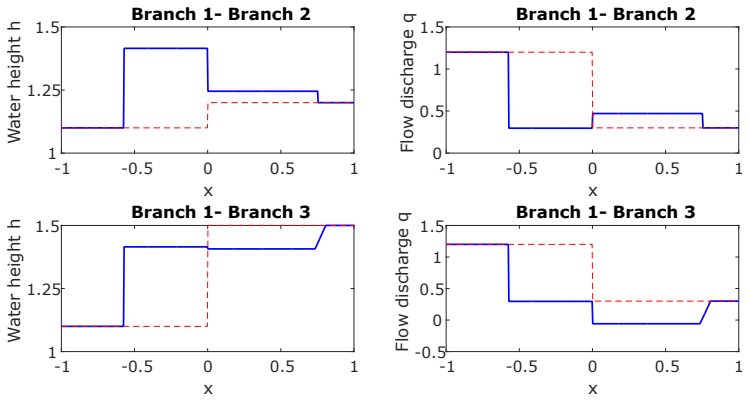

Fig. 11. Water height and flow discharge evolution for junction Riemann solution in non symmetric with small forward bottom discontinuities (e.g., $z_1 = 0.0$, $z_2 = z_3 = 0.1$) at $t = 0.2[s]$.

Example 4.5. Consider the following initial data with large forward bottom discontinuities with $r = 0.75$. The widths $b_1 = 1$, $b_2 = 0.9$, and $b_3 = 0.5$ are considered.

$$v_{1l} = \begin{bmatrix} 1.1 \\ 1.2 \\ 0.0 \end{bmatrix}, \quad v_{2r} = \begin{bmatrix} 1.2 \\ 0.3 \\ 0.4 \end{bmatrix}, \quad v_{3r} = \begin{bmatrix} 1.3 \\ 0.3 \\ 0.4 \end{bmatrix}. \tag{4.5}$$

Under a large forward bottom discontinuities: Figure 12 shows that condition (3.67)

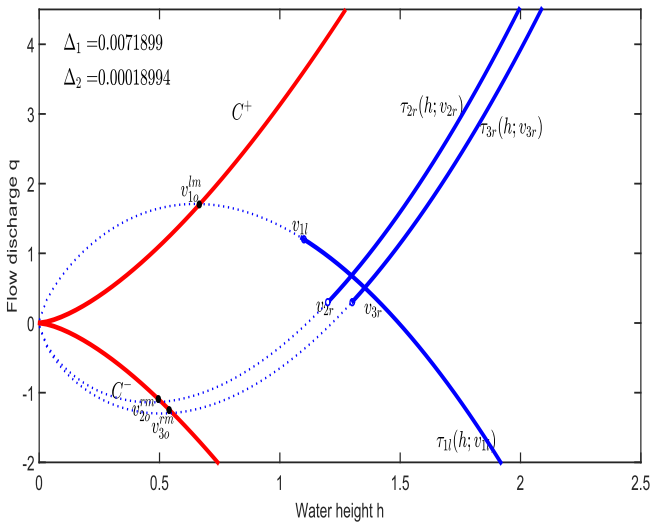

Fig. 12. The solution of the junction Riemann problem with large forward bottom discontinuities (e.g., $z_1 = 0.0$, $z_2 = z_3 = 0.4$) and $r = 0.75$.

and condition (3.23) are not satisfied and therefore there is not a solution. These examples are illustrated the direct effect of condition (3.67) and condition (3.23) on the existence of the Riemann solution.

5. Summary and conclusion

In this work, we have studied the existence and uniqueness of the solution of the nonlinear Riemann problem in three rectangular channels network without assuming special hypothesis except the sub-critical flow condition. The analysis is made challenging by the presence of bottom discontinuities and width variations between the channels forming the junction. Working on the conservation of the mass and total head at the junction, we have given the existence domain of the solution in terms of relationships between the amplitude of the bottom discontinuities, the ratio of the channels widths, and the discharge allocation. Working on the relations between quantities across the rarefaction and shock waves we have completed the existence analysis. The physical meaning of each relationship is clearly stated and analyzed in this work.

The overall result can open the door to the application of the nonlinear junction Riemann solution in practical simulation of open channels networks allowing the definition of physically sound internal boundaries between channels. Justifying the

use of this Riemann solution in the internal boundaries definition thought the comparison with alternative strategies and the validation against experimental are the topics of future work.

Acknowledgments

The first author is grateful for financial support from the Egyptian Ministry of Higher Education (MOHE: 2014/2018) and by the National Authority for Remote Sensing and Space Sciences (NARSS).

References

[1] M. Briani, B. Piccoli and J.-M. Qiu, Notes on RKDG Methods for Shallow-Water Equations in Canal Networks, *Journal of Scientific Computing* (2015) 1–23.

[2] J. J. Stoker, *Water waves: The mathematical theory with applications* (John Wiley & Sons, 2011).

[3] M. Garavello and B. Piccoli, Traffic flow on a road network using the aw–rascle model, *Communications in Partial Differential Equations* **31**(2) (2006) 243–275.

[4] L. O. Müller and P. J. Blanco, A high order approximation of hyperbolic conservation laws in networks: Application to one-dimensional blood flow, *Journal of Computational Physics* **300** (2015) 423–437.

[5] T. Sturm and J. Tuzson, Open channel hydraulics, *Applied Mechanics Reviews* **54** (2001) p. 107.

[6] J. A. Cunge, F. M. Holly and A. Verwey, Practical aspects of computational river hydraulics (1980).

[7] P. M. Jacovkis, One-Dimensional Hydrodynamic Flow in Complex Networks: State of the Art, Some Applications and Generalizations, in *Southern Hemisphere Paleo-and Neoclimates*, (Springer, 2000) pp. 17–25.

[8] Y. Zhang, Simulation of open channel network flows using finite element approach, *Communications in Nonlinear Science and Numerical Simulation* **10**(5) (2005) 467–478.

[9] G. Kesserwani, R. Ghostine, J. Vazquez, R. Mosé, M. Abdallah and A. Ghenaim, Simulation of subcritical flow at open-channel junction, *Advances in Water Resources* **31**(2) (2008) 287–297.

[10] R. Ghostine, R. Mose, J. Vazquez, A. Ghenaim and C. Grégoire, Two-dimensional simulation of subcritical flow at a combining junction: luxury or necessity?, *Journal of Hydraulic Engineering* **136**(10) (2010) 799–805.

[11] R. Ghostine, J. Vazquez, A. Terfous, R. Mose and A. Ghenaim, Comparative study of 1D and 2D flow simulations at open-channel junctions, *Journal of Hydraulic Research* **50**(2) (2012) 164–170.

[12] K.-H. Chang, T.-J. Chang and Y.-M. Chiang, A novel SPH-SWEs approach for modeling subcritical and supercritical flows at open channel junctions, *Journal of Hydro-environment Research* (2015).

[13] M. B. Abbott, An introduction to the method of characteristics (1966) 209–214.

[14] H. Elhanafy and G. Copeland, Modified method of characteristics for the shallow water equations, in *2nd IMA International Conference on flood Risk Assessment*, 2007.

[15] M. Garcia-Navarro and J. Saviron, Numerical simulation of unsteady flow at open channel junctions, *Journal of hydraulic research* **30**(5) (1992) 595–609.

[16] A. O. Akan and B. C. Yen, Diffusion-wave flood routing in channel networks, *Journal of the Hydraulics Division* **107**(6) (1981) 719–732.
[17] S. K. Gurram, K. S. Karki and W. H. Hager, Subcritical junction flow, *Journal of Hydraulic Engineering* **123**(5) (1997) 447–455.
[18] C.-C. Hsu, W.-J. Lee and C.-H. Chang, Subcritical open-channel junction flow, *Journal of Hydraulic Engineering* **124**(8) (1998) 847–855.
[19] S. Shabayek, P. Steffler and F. Hicks, Dynamic model for subcritical combining flows in channel junctions, *Journal of Hydraulic Engineering* **128**(9) (2002) 821–828.
[20] C. E. Rice, Open channel junctions with supercritical flow, *ARS-United States Department of Agriculture, Agricultural Research Service (USA)* (1985).
[21] G. C. Christodoulou, Incipient hydraulic jump at channel junctions, *Journal of Hydraulic Engineering* **119**(3) (1993) 409–423.
[22] G. Kesserwani, R. Ghostine, J. Vazquez, A. Ghenaim and R. Mosé, One-dimensional simulation of supercritical flow at a confluence by means of a nonlinear junction model applied with the rkdg2 method, *International journal for numerical methods in fluids* **57**(12) (2008) 1695–1708.
[23] A. S. Ramamurthy, L. B. Carballada and D. M. Tran, Combining open channel flow at right angled junctions, *Journal of Hydraulic Engineering* **114**(12) (1988) 1449–1460.
[24] M. S. Goudiaby and G. Kreiss, A Riemann problem at a junction of open canals, *Journal of Hyperbolic Differential Equations* **10**(03) (2013) 431–460.
[25] F. Alcrudo and F. Benkhaldoun, Exact solutions to the Riemann problem of the shallow water equations with a bottom step, *Computers & Fluids* **30**(6) (2001) 643–671.
[26] R. Bernetti, V. A. Titarev and E. F. Toro, Exact solution of the Riemann problem for the shallow water equations with discontinuous bottom geometry, *Journal of Computational Physics* **227**(6) (2008) 3212–3243.
[27] P. G. LeFloch, *Hyperbolic Systems of Conservation Laws: The theory of classical and nonclassical shock waves* (Springer Science & Business Media, 2002).
[28] R. M. Colombo and M. Garavello, On the Cauchy problem for the p-system at a junction, *SIAM Journal on Mathematical Analysis* **39**(5) (2008) 1456–1471.
[29] R. M. Colombo, M. Herty and V. Sachers, On 2\times2 conservation laws at a junction, *SIAM Journal on Mathematical Analysis* **40**(2) (2008) 605–622.
[30] F. M. Henderson, *Open channel flow* (Macmillan, 1996).
[31] A. Valiani and V. Caleffi, Depth–energy and depth–force relationships in open channel flows: analytical findings, *Advances in Water Resources* **31**(3) (2008) 447–454.
[32] R. J. LeVeque, *Numerical methods for conservation laws* (Springer, 1992).
[33] B. Ramana, *Higher Engineering Mathematics*, no. 1.14-1.15 (Tata McGraw-Hill Education, 2006).
[34] M. J. Powell, A hybrid method for nonlinear equations, *Numerical methods for nonlinear algebraic equations* **7** (1970) 87–114.